


2015

Gadolinium Modifies the Cell Membrane to Inhibit Permeabilization by Nanosecond Electric Pulses

Elena C. Gianulis
Old Dominion University

Andrei G. Pakhomov
Old Dominion University

Follow this and additional works at: https://digitalcommons.odu.edu/bioelectrics_pubs

 Part of the [Biophysics Commons](#), and the [Medical Biophysics Commons](#)

Repository Citation

Gianulis, Elena C. and Pakhomov, Andrei G., "Gadolinium Modifies the Cell Membrane to Inhibit Permeabilization by Nanosecond Electric Pulses" (2015). *Bioelectrics Publications*. 157.
https://digitalcommons.odu.edu/bioelectrics_pubs/157

Original Publication Citation

Gianulis, E. C., & Pakhomov, A. G. (2015). Gadolinium modifies the cell membrane to inhibit permeabilization by nanosecond electric pulses. *Arch Biochem Biophys*, 570, 1-7. doi:10.1016/j.abb.2015.02.013



HHS Public Access

Author manuscript

Arch Biochem Biophys. Author manuscript; available in PMC 2016 March 15.

Published in final edited form as:

Arch Biochem Biophys. 2015 March 15; 570: 1–7. doi:10.1016/j.abb.2015.02.013.

Gadolinium modifies the cell membrane to inhibit permeabilization by nanosecond electric pulses

Elena C. Gianulis^{*} and Andrei G. Pakhomov

Frank Reidy Research Center for Bioelectrics, Old Dominion University, Norfolk, VA, 23508, USA

Abstract

Lanthanide ions are the only known blockers of permeabilization by electric pulses of nanosecond duration (nsEP), but the underlying mechanisms are unknown. We employed timed applications of Gd^{3+} before or after nsEP (600-ns, 20 kV/cm) to investigate the mechanism of inhibition, and measured the uptake of the membrane-impermeable YO-PRO-1 (YP) and propidium (Pr) dyes. Gd^{3+} inhibited dye uptake in a concentration-dependent manner. The inhibition of Pr uptake was always about 2-fold stronger. Gd^{3+} was effective when added after nsEP, as well as when it was present during nsEP exposure and removed afterwards. Pores formed by nsEP in the presence of Gd^{3+} remained quiescent unless Gd^{3+} was promptly washed away. Such pores resealed (or shrunk) shortly after the wash despite the absence of Gd^{3+} . Finally, a brief (3 s) Gd^{3+} perfusion was equally potent at inhibiting dye uptake when performed either immediately before or after nsEP, or early before nsEP. The persistent protective effect of Gd^{3+} even in its absence proves that inhibition by Gd^{3+} does not result from simple pore obstruction. Instead, Gd^{3+} causes lasting modification of the membrane, occurring promptly and irrespective of pore presence; it makes the membrane less prone to permeabilization and/or reduces the stability of electropores.

Keywords

Electroporation; Nanosecond electric pulses; Gadolinium; Lanthanide ions

Introduction

The phenomenon that high-voltage intense electric pulses of nanosecond duration (nsEP) cause cell membrane permeabilization, or electroporation, has been well studied in recent decades (1, 2). In addition to plasma membrane permeabilization, nsEP can lead to cell swelling and blebbing (3, 4) and activation of necrotic and apoptotic cell death pathways (5–7). An important quality of pores formed by nsEP is that the diameter is thought to be no larger than approximately 1 – 1.5 nm (“nanopores”). This size parameter was determined

© 2015 Published by Elsevier Inc.

^{*}Corresponding author: Elena C. Gianulis, Ph.D., Frank Reidy Center for Bioelectrics, Old Dominion University, 4211 Monarch Way, Suite 300, Norfolk, VA 23508, USA, (757)-683-2234, Fax: (757)-451-1010, egianulis@odu.edu, egianulis@gmail.com.

Publisher's Disclaimer: This is a PDF file of an unedited manuscript that has been accepted for publication. As a service to our customers we are providing this early version of the manuscript. The manuscript will undergo copyediting, typesetting, and review of the resulting proof before it is published in its final citable form. Please note that during the production process errors may be discovered which could affect the content, and all legal disclaimers that apply to the journal pertain.

experimentally by the selective uptake of smaller dye molecules, such as YO-PRO-1 (YP) and ions (such as Tl^+) versus larger dye molecules, such as propidium (Pr) (8, 9), as well as by the blockage of cell swelling using solutes that are too large to pass through the pores (3). Finally, pores formed by nsEP are stable with a lifetime as long as several minutes (1, 8, 10, 11).

To date, lanthanide ions, such as gadolinium (Gd^{3+}), are the only known inhibitors of electropermeabilization (4, 12). Gd^{3+} was shown to attenuate the effects of nsEP, reducing cell swelling and blebbing, and increased cell survival (12). However, the details and mechanism of Gd^{3+} block of electropermeabilization are poorly understood.

Lanthanide ions are well-known nonspecific inhibitors of several types of voltage-gated and mechanosensitive ion channels, as well as ion transporters and membrane-bound receptors (13–15). Though the mechanism of inhibition by lanthanide ions is not clear, it is thought to be due to their similar cationic radii with that of calcium (Ca^{2+}) ions (16). On the other hand, there is evidence that lanthanide ions can bind to phospholipids with high affinity and affect the physical properties of the lipid bilayer, altering the function of membrane-bound proteins (17–19). Therefore, it remains a controversy how lanthanide ions are such potent nonspecific inhibitors of ion channels, transporters, and receptors.

Understanding the inhibitory effect of Gd^{3+} on electropermeabilization can help to uncover a broader mechanism of Gd^{3+} 's action on the cell membrane and, in turn, on membrane-bound proteins. It is unclear whether Gd^{3+} clogs pores that are formed by nsEP or if it alters the plasma membrane to interfere with pore formation and/or stability. In the present study, we sought to investigate the inhibitory mechanism of Gd^{3+} on electropermeabilization. Our results revealed a persistent and sustained protection of cells from nsEP by Gd^{3+} , even when Gd^{3+} ions were absent in the solution. These findings prove that Gd^{3+} does not clog pores that are formed by nsEP. Instead, Gd^{3+} causes a lasting modification of the plasma membrane, which occurs independently of pore presence. Thus, the membrane becomes less susceptible to permeabilization, and pores that are formed are less stable.

Materials and Methods

Cell Culture

Chinese hamster ovary cells (CHO-K1) cells were obtained from the American Type Culture Collection (ATCC, Manassas, VA). Cells were maintained in culture at 37°C, 5% CO_2 in Ham's F12K Media supplemented with 10% fetal bovine serum and 1% penicillin/streptomycin. The media and its components were purchased from Mediatech Cellgro (Herndon, VA), except for the serum which was purchased from Atlanta Biologicals (Norcross, GA). One day prior to experiments, cells were passaged and transferred onto glass coverslips (#0 thickness, 12mm diameter) pretreated with poly-L-lysine (Sigma-Aldrich, St. Louis, MO) to improve cell adhesion.

Cell Imaging and Dye Uptake Measurements

A coverslip with cells was placed in a glass-bottomed chamber (Warner Instruments, Hamden, CT) mounted on an Olympus IX71 inverted microscope equipped with an FV

1000 confocal laser scanning system (Olympus America, Center Valley, PA). The chamber was filled with a physiological solution containing (in mM): 140 NaCl, 5 KCl, 2 MgCl₂, 2 CaCl₂, 1 HEPES, 10 Glucose, X GdCl₃, (pH 7.4 with NaOH) where X was varied from 0 to 1 mM. The concentration of HEPES was kept at a minimum to prevent precipitation of Gd³⁺ in the solution. The osmolality of the solution was between 290 and 310 mOsm/kg, as measured by a freezing point microosmometer (Advanced Instruments, Inc., Norwood, MA). The membrane-impermeable fluorescent dyes YP and Pr iodide were added to the solution at 1 μM and 5 μg/mL, respectively. These dyes are non-fluorescent when in the chamber solution, but once they enter the cell, their emission increases profoundly upon binding to intracellular nucleic acids (20). All chemicals were purchased from Sigma-Aldrich and Life Technologies (Grand Island, NY). Where indicated in the text, the chamber was continuously perfused with the physiological solution (including the dyes) during the experiment, with a flow rate of 3 mL/min. All experiments were performed at room temperature (22 ± 2°C).

Differential-interference contrast (DIC) and fluorescent images were taken with a 40X, NA 0.95 dry objective as a time series beginning before nsEP exposure and continuing for up to 7 minutes after it. YP was excited with a blue laser (488 nm) and Pr was excited with a green laser (543 nm); the emission of each dye was detected between 505 and 525 nm or between 560 and 660 nm, respectively. To avoid “cross-talk” between the dyes, the lasers were operated in a line sequence mode. Images were quantified using MetaMorph Advanced v.7.7.0.0 (Molecular Devices, Foster City, CA).

Fast-Step Solution Delivery

Direct application of Gd³⁺ to the cells (Figures 2 and 5) was done using a fast-step SF-77B perfusion system connected to a VC-6 valve controller (Warner Instruments, Hamden, CT). Briefly, we combined the continual solution flow through the chamber with timed application of the solution directly to studied cells via a 3-barrel glass capillary assembly. Two of the barrels were each filled with the physiological solution including the fluorescent dyes, one with 250 μM GdCl₃ added and the other containing 0 μM GdCl₃. With the chamber solution flowing, these capillaries were positioned upstream from the cells so that a flow of solution from the barrels, when the valves were open, would go to an area adjacent to the cells, but not reaching the cells. The opening of the valves was controlled by a timed TTL pulse (see below), allowing the solution to flow down the capillary by gravity at ~ 900 μL/min. The solution with Gd³⁺ (or the control solution in the other barrel) was applied to the cells precisely 2 s after opening the valve by an abrupt move of the respective barrel with a stepping mechanism so that the flow of solution was redirected to the cells. After a designated time (3 or 5 s), the barrel was moved back and the valve was closed to cease the perfusion from the barrel. The solution flow through the chamber continued for the duration of the experiment, thus washing away Gd³⁺. Hence, the fast-step delivery system allowed for application of undiluted Gd³⁺ directly to the studied cells for precisely and only the designated time interval. Control solution was delivered in the same way to determine that no mechanical artifacts were produced from this system.

NsEP Exposure

NsEP were delivered to the cells as previously described (10). Briefly, nearly rectangular 600 ns pulses were generated in a transmission line-type circuit upon delivery of a TTL trigger pulse from pClamp software via a Digidata 1322A output (Molecular Devices). The same software and Digidata output were used to synchronize nsEP exposure, image acquisition, and chamber and fast-step perfusion. NsEP were delivered to a selected cell or small group of cells with a pair of tungsten rod electrodes (100 μm diameter, $\sim 100 \mu\text{m}$ gap) at a rate of 2 pulses/s. Delivery of nsEP to the cells was delayed until 28 s after the beginning of the image acquisition sequence so that several baseline images were recorded prior to exposure. The electrodes were positioned precisely 30 μm above the coverslip using a robotic manipulator (MP-225, Sutter Instruments, Novato, CA) so that the selected cell(s) was positioned in the middle of the gap between the electrode tips. The electric field (EF) at the cell location between the electrodes was determined by 3D simulations with a finite-element Maxwell equation solver Amaze 3D (Field Precision, Albuquerque, NM), as described previously (10). In all experiments, the EF amplitude was 20 kV/cm. In each experiment, the number of pulses ranged from 2 to 10, which resulted in differential dye uptake. In turn, the emission detector (photomultiplier tube) sensitivity was adjusted accordingly. Therefore, the emission curves from different sets of experiments should not be compared as their Y-axes (in arbitrary units, a.u.) are not the same.

Statistical Analysis

Data are presented as mean \pm s.e. Statistical analyses were performed using a two-tailed *t*-test where $p < 0.05$ was considered statistically significant.

Results

Gd³⁺ inhibits nsEP-induced uptake of YP and Pr in a concentration-dependent manner

The first series of experiments investigated the concentration range over which Gd³⁺ protects cells from the effects of nsEP-induced membrane permeabilization. CHO-K1 cells were bathed in a physiological solution containing varying concentrations of Gd³⁺, ranging from 0 to 1000 μM . Following nsEP exposure (10 pulses), we observed a significant increase in both YP and Pr emission in cells bathed in 0 μM Gd³⁺ (“control”, Figure 1A & B). Incrementally increasing the concentration of Gd³⁺ up to 1000 μM progressively decreased the dye uptake after nsEP exposure. Pr emission was significantly reduced to ~ 50 % of control by 100 μM Gd³⁺ ($p < 0.05$; Figure 1B & C), whereas at the same concentration, YP emission was only slightly less than control and not significantly different ($p > 0.05$) (Figure 1A & C). From 250 to 1000 μM Gd³⁺, the uptake of both YP and Pr after nsEP exposure was profoundly reduced with emission ~ 20 % of control ($p < 0.01$; Figure 1A-D). Interestingly, by 20 seconds after nsEP exposure, the uptake of both YP and Pr reached a plateau, indicating dye uptake was stopped and there were no more pores open through which the dyes could diffuse. It is unclear whether this was due to Gd³⁺ clogging the existing pores or inducing the formed pores to reseal.

In addition to reducing dye uptake, we observed a significant effect of Gd³⁺ on cell morphological changes following nsEP (Figure 1D). Cells that were bathed in 250 μM Gd³⁺

exhibited noticeably less swelling than those that were in 0 μM Gd^{3+} , consistent with our previous findings (4, 12). Altogether, these data confirm that Gd^{3+} is a strong inhibitor of dye uptake and cell swelling induced by nsEP. Further, we show that the uptake of Pr is more strongly reduced than that of YP, which may be due to the slightly larger size of the Pr molecule. Therefore, it is possible that Gd^{3+} has a greater inhibitory effect on the transport of larger molecules. However, from these results we still cannot distinguish whether Gd^{3+} is clogging nsEP-induced pores or is somehow altering the plasma membrane.

Brief exposure of cells to Gd^{3+} profoundly reduces nsEP-induced uptake of YP and Pr

We next asked whether the inhibitory effect of Gd^{3+} on dye uptake requires Gd^{3+} to be present at the time of nsEP exposure, and if it can inhibit molecular transport through already formed electropores. Cells were exposed to a train of 4 nsEP at 28 s (dashed line in Figure 2), followed from 31 to 36 s by a fast-step perfusion with the solution containing either 250 or 0 μM Gd^{3+} (red arrow in Figure 2). We decreased the number of pulses from the previous experiment, as we determined that a lower dose was sufficient to electropermeabilize the membrane. We found that this transient application of Gd^{3+} resulted in a significant ($p < 0.001$) reduction in both YP and Pr uptake. Notably, Pr emission was reduced by ~ 9 -fold at 300 s, versus a ~ 3.5 -fold reduction in YP emission at 300 s. We asked whether this reduction in emission was simply due to the “missed” dye uptake during the 5 second period when Gd^{3+} was delivered to the cells. By 300 s, the uptake of YP and Pr was reduced by ~ 486 and ~ 87 a.u., respectively, which was much greater than the “missed” uptake during the period of Gd^{3+} perfusion (~ 70 and ~ 5 a.u., respectively). Thus, the reduction in emission was not due to the “missed” uptake. Rather, Gd^{3+} caused continued inhibition of dye uptake despite being washed away, suggesting that either Gd^{3+} had enough time to clog and/or reseal the pores during the brief perfusion, or that it was not fully washed away. These data indicate that the inhibitory effect of Gd^{3+} does not depend on its presence at the time of nsEP exposure, and it is sustained even after its removal. Finally, since Pr is slightly larger than YP, the greater inhibition of Pr transport may be indicative of the reduction of the mean diameter of nsEP-opened pores by Gd^{3+} .

The presence of Gd^{3+} does not prevent pore formation by nsEP, but the pores remain quiescent

The previous experiments prompted us to ask 1) if Gd^{3+} prevents pore formation by nsEP and 2) if pores are formed, whether molecular transport through the permeabilized membrane can be restored upon removing Gd^{3+} ? Cells were bathed in physiological solution containing either 0 or 250 μM Gd^{3+} and exposed to 4 nsEP at 28 s. Beginning at either 31 or 51 s, the chamber bath perfusion was activated so that the solution containing 0 μM Gd^{3+} was flowing, thus washing away Gd^{3+} . We observed a modest recovery in uptake of both YP and Pr when the wash began immediately following nsEP (at 31 s), which was ~ 2.5 – 3-fold greater than when the wash was delayed for 20 s (Figure 3). However, even with this modest recovery, the emission of YP and Pr was still significantly reduced (~ 2.6 -fold and 5-fold less than 0 Gd^{3+} at 300 s, respectively), indicating that the inhibitory effect of Gd^{3+} persisted after it had been washed away. Inhibition of Pr uptake was always ~ 2 -fold greater than YP regardless of whether the wash was immediate or delayed for 20 s. Notably, by 100 s, the emission for both YP and Pr reached a plateau, indicating there was no additional dye

uptake through the pores. This plateau is similar to that seen in Figure 1, except in this case, it was well after Gd^{3+} had been washed out of the bath. Because Gd^{3+} was washed away by this time, the plateau of dye uptake was clearly not due to Gd^{3+} clogging pores, but rather indicates a rapid shrinking and/or resealing of pores as a delayed effect of Gd^{3+} . It is possible that there may be some Gd^{3+} bound to the membrane that did not get washed away. However, this membrane-bound Gd^{3+} would be unavailable to clog pores due to tight binding, and the concentration of any remaining Gd^{3+} in the solution would be far less than the 100 μM concentration needed to inhibit dye uptake (see Figure 1). Therefore, these data indicate that 1) pores do form in the presence of Gd^{3+} , 2) Gd^{3+} provides sustained inhibition of molecular transport, and 3) Gd^{3+} has delayed effects long after it has been removed inducing pores to shrink or reseal. These results suggest that Gd^{3+} is not clogging pores, but rather is somehow modifying the plasma membrane so that membrane permeability is profoundly reduced.

To test this notion, we conducted a similar experiment in which cells bathed in physiological solution containing either 0 or 250 μM Gd^{3+} were exposed to a pair of nsEP at 28 s (“2p”, first dashed line, Figure 4), followed by a wash with 0 μM Gd^{3+} beginning at 30 s. Then, 3 minutes after the first nsEP exposure, a second pair of nsEP were delivered (“2p+2p”, second dashed line, Figure 4) to measure the formation of new pores with Gd^{3+} absent. Thus, the total number of nsEP delivered in the 2p+2p group was a split fraction of the nsEP train from the previous experiment.

We found when cells not treated with Gd^{3+} (0 Gd^{3+}) were exposed to two trains of nsEP, the second nsEP exposure elicited a much stronger effect (Figure 4). Emission of both YP and Pr were increased by ~ 2-fold and ~ 4-fold, respectively, relative to a single exposure of nsEP. This is consistent with what we previously reported (21, 22), in which cells exposed to nsEP become electrosensitized to subsequent nsEP, thereby eliciting an overall enhanced effect. In contrast, cells that were bathed in Gd^{3+} at the beginning of the experiment exhibited an increase in both YP and Pr emission after the second nsEP exposure, indicating new pores had been formed. However, the magnitude of YP and Pr uptake induced by the second nsEP exposure was ~ 2.7-fold and ~ 11-fold less than the 0 Gd^{3+} group, respectively. These data demonstrate that Gd^{3+} has a sustained inhibitory effect, reducing the effects of subsequent nsEP exposures even in its absence. Furthermore, the greater inhibition of transport of the slightly larger Pr molecule after the second nsEP exposure is consistent with the notion that Gd^{3+} is limiting the mean diameter of the electropores. Thus, these findings support the proposed mechanism that Gd^{3+} is modifying the physical properties of the plasma membrane which is sustained even in its absence.

Gd^{3+} causes lasting modification the plasma membrane irrespective of the presence of electropores

If the mechanism of Gd^{3+} inhibition of nsEP-induced dye uptake is indeed long-lasting modification of the plasma membrane, then one might presume that treatment of cells with Gd^{3+} at any point before or after nsEP exposure would result in a reduction in membrane permeability. To test this, we transiently applied a solution containing either 0 or 250 μM Gd^{3+} to the cells via fast-step perfusion for varying times (see Materials and Methods) –

from 3–6 s (A), 25–28 s (B), 31–34 s (C), or 91–94 s (D; red arrows in Figure 5) – before or after nsEP exposure at 28 s (4 pulses; dashed lines in Figure 5).

Brief perfusion of Gd^{3+} immediately before (from 25–28 s; Figure 5B) or after nsEP (from 31–34 s; Figure 5C), as well as early before nsEP (from 3–6 s; Figure 5A), all resulted in a robust reduction in uptake of both YP and Pr. Pr uptake was more strongly inhibited than YP, with an average ~ 6-fold reduction in Pr emission compared to an average ~ 2-fold reduction in YP emission. Most notably, each dyes' emission was reduced by the same magnitude compared to their respective controls regardless of whether Gd^{3+} was transiently applied from 3–6 s, 25–28 s, or 31–34 s. Because no pores had been formed at the delivery times that preceded nsEP, this indicates that Gd^{3+} does not clog nsEP-induced pores to inhibit membrane permeability. Rather, this finding demonstrates that Gd^{3+} causes lasting modification of the plasma membrane that inhibits later nsEP-induced dye uptake. Furthermore, these findings reveal that the mechanism of Gd^{3+} inhibition does not depend on the presence of electropores in order for it to impose its effects on the plasma membrane. Therefore, this suggests that Gd^{3+} makes the membrane less susceptible to permeabilization, and reduces the size and/or permeability of formed electropores.

Finally, brief application of Gd^{3+} to the cells well after nsEP exposure (from 91–94 s) resulted in an immediate slowing in the rate of dye uptake for both YP and Pr (Figure 5D). Interestingly, the rate of dye uptake after perfusion of Gd^{3+} from 91–94 s is similar to the rate of uptake when it was applied from 3–6 s, 25–28 s, or 31–34 s. This finding indicates that the inhibitory effect of Gd^{3+} is the same regardless of when it is applied.

Discussion

In this study, we investigated how Gd^{3+} protects cells from the effects of nsEP-induced permeabilization. Does Gd^{3+} clog nsEP-induced pores formed in the plasma membrane? Or does it modify the plasma membrane to interfere with pore formation and/or stability? Here we show that Gd^{3+} inhibits uptake of both YP and Pr in a dose-dependent manner, with a ~ 2-fold greater inhibition of Pr uptake. We found that Gd^{3+} inhibition of dye uptake is persistent, being sustained even when Gd^{3+} is absent in the solution. Finally, transient application of Gd^{3+} either immediately before or after nsEP, as well as early before nsEP, reduced dye uptake to a similar extent. From our results, we can conclude that the inhibitory effect of Gd^{3+} is not by clogging nsEP-induced pores. Rather, Gd^{3+} causes lasting modification of the plasma membrane that occurs rapidly and irrespective of pore presence. Thus, Gd^{3+} makes the plasma membrane less susceptible to electropermeabilization and decreases pore size and/or lifetime.

Our findings prompted us to ask how Gd^{3+} may be modifying the plasma membrane to inhibit electropermeabilization. There is a great deal of evidence that polyvalent cations (including La^{3+} , Gd^{3+} , Tb^{3+} , Cd^{2+} , Be^{2+} , Ca^{2+} , Mn^{2+} , Ba^{2+} , Sr^{2+} , and Mg^{2+}) increase the surface tension of the lipid bilayer (17–19, 23–31). This occurs by penetration of the polyvalent cations deep within the hydrophilic region of the bilayer due to their high affinity binding to charged phospholipids, such as phosphatidylserine (23, 25, 29, 32), as well as to zwitterionic phospholipids, such as phosphatidylcholine and phosphatidylethanolamine (18,

28, 30, 33). The cations subsequently dehydrate the phospholipid headgroups, making the membrane surface more hydrophobic (23, 26, 28, 29, 34). Consequently, Akuzawa-Tateyama, et al. suggested that the increased membrane hydrophobicity caused by La^{3+} may accelerate electropore closure (35). In support of this idea, molecular dynamics simulations show that Ca^{2+} decreases both the size and lifetime of electropores, presumably by forming a Ca^{2+} -lipid complex (36). In this study, we found that Gd^{3+} induces electropores to rapidly reseal or shrink (see Figures 1 and 3). Furthermore, we show that Gd^{3+} is equally potent at inhibiting dye uptake regardless of whether it was transiently applied early before, immediately before, or immediately after nsEP (Figure 5), indicating that the effect of Gd^{3+} on the plasma membrane is independent of the presence of electropores. Therefore, the results from our study suggest that Gd^{3+} may inhibit electroporemeabilization by increasing membrane tension due to high affinity binding to phospholipids, consistent with previously reported effects of polyvalent cations on the plasma membrane (17–19, 23–31). We can surmise that this increased tension would result in fewer nsEP-induced pores overall in the membrane and/or decreased stability of the pores that are formed. Additionally, this may result in an overall reduction in the mean diameter of electropores, thus explaining the differential inhibition of transport between YP and the slightly larger Pr molecule that we observed.

The effect of polyvalent cations on the lipid bilayer goes beyond the bilayer itself, but also affects membrane-bound proteins that are modulated by membrane fluidity and surface potential. Lanthanide ions, such as Gd^{3+} , are known inhibitors of several types of ion channels, including voltage-gated calcium channels, stretch-activated ion channels, as well as Ca^{2+} - and Mg^{2+} -ATPases and the $\text{Na}^+/\text{Ca}^{2+}$ -exchanger (13, 15, 16, 19, 37–39). Though the mechanism of inhibition by lanthanide ions is not completely clear, it is thought to be due to their similar cationic radii with Ca^{2+} ions, and competing with the permeant ions for a binding site in the selectivity filter of the channel (40–42). However, a competing theory suggests that compaction of the phospholipids in the plasma membrane by Gd^{3+} produces lateral pressure on the membrane-bound ion channels, thus shifting their equilibrium to the closed state (17, 19). Our work here reveals an effect of Gd^{3+} on the plasma membrane, which we propose is by an increase in membrane tension. Our results, coupled with previous findings, support the latter theory of modification of the plasma membrane as the primary mechanism of lanthanide inhibition of ion channels. Furthermore, given the broad range of cations that modify the lipid bilayer (17, 19, 23, 25) and have been shown to decrease channel conductance (17, 19), it is reasonable to think that this may be a universal mechanism of inhibition of ion channels by a number of multivalent cations.

In this study, we used high-intensity nsEP to permeabilize the plasma membrane. Another method of electroporemeabilizing the cell is to impose an EF using voltage-clamp commands to hyperpolarize the membrane (35, 43–45). Interestingly, the pores created by hyperpolarization have similar conductive properties to nsEP-induced pores (10), including an inward current, voltage sensitivity, and ion selectivity. The hyperpolarization-induced inward currents (I_{ep}) were inhibited by lanthanum ions (La^{3+}) in the concentration range of 0.1 to 0.5 mM La^{3+} (35, 43–45). This effective concentration range of La^{3+} inhibition of I_{ep} is in good agreement with what we observed previously (4, 12) and in the present study, in which Gd^{3+} concentrations from 0.1 mM to 1 mM inhibited nsEP-induced permeabilization.

Thus, these similarities suggest that the pores created in the cell membrane by high-intensity EFs from either nsEP or hyperpolarizing voltage-clamp commands may in fact be the same entity, and may both be inhibited by lanthanide ions via the same mechanism.

In summary, we conclude that Gd^{3+} inhibits nsEP-induced permeabilization not by clogging electropores. Rather, it causes lasting modification of the plasma membrane, which occurs promptly and irrespective of electropore presence. This modification makes the membrane less prone to electroporation and decreases the permeability and/or stability of electropores that are formed. Our conclusions can have a broader application on our understanding of the effects of polyvalent cations on the plasma membrane and membrane-bound proteins. Finally, previous studies have shown cytoprotection by lanthanide ions in the liver from toxic products of xenobiotic biotransformation (16). Together with our findings, this suggests that lanthanide ions may have a broader protective effect in other cell membrane injury models.

Acknowledgments

This work was supported by R01GM088303 from the National Institute of General Medical Sciences (to AGP). We thank Dr. S. Xiao (Old Dominion University, Norfolk, VA) for continued help with nsEP exposure and dosimetry.

Abbreviations

DIC	differential-interference contrast
EF	electric field
Gd³⁺	gadolinium ion
nsEP	nanosecond electric pulses
Pr	Propidium
YP	YO-PRO-1

References

1. Pakhomov, AG.; Pakhomov, ON. *Advanced Electroporation Techniques in Biology and Medicine*. Pakhomov, AG.; Miklavcic, D.; Markov, MS., editors. CRC Press; Boca Raton: 2010. p. 177-194.
2. Schoenbach KH, Hargrave B, Joshi RP, Kolb JF, Nuccitelli R, Osgood C, Pakhomov A, Stacey M, Swanson RJ, White JA, Xiao S, Zhang J, Beebe SJ, Blackmore PF, Buescher ES. *Ieee Transactions on Dielectrics and Electrical Insulation*. 2007; 14:1088–1109.
3. Nesin OM, Pakhomova ON, Xiao S, Pakhomov AG. *Biochimica et biophysica acta*. 2011; 1808:792–801. [PubMed: 21182825]
4. Pakhomov AG, Shevin R, White JA, Kolb JF, Pakhomova ON, Joshi RP, Schoenbach KH. *Arch Biochem Biophys*. 2007; 465:109–118. [PubMed: 17555703]
5. Ibey BL, Pakhomov AG, Gregory BW, Khorokhorina VA, Roth CC, Rassokhin MA, Bernhard JA, Wilmlink GJ, Pakhomova ON. *Biochimica et biophysica acta*. 2010; 1800:1210–1219. [PubMed: 20691249]
6. Pakhomova ON, Gregory B, Semenov I, Pakhomov AG. *Biochimica et biophysica acta*. 2014; 1838:2547–2554. [PubMed: 24978108]
7. Morotomi-Yano K, Akiyama H, Yano K. *Biochemical and biophysical research communications*. 2013; 438:557–562. [PubMed: 23899527]

8. Bowman AM, Nesin OM, Pakhomova ON, Pakhomov AG. *The Journal of membrane biology*. 2010; 236:15–26. [PubMed: 20623351]
9. Vernier PT, Sun Y, Gundersen MA. *BMC Cell Biol*. 2006; 7:37. [PubMed: 17052354]
10. Pakhomov AG, Bowman AM, Ibey BL, Andre FM, Pakhomova ON, Schoenbach KH. *Biochemical and biophysical research communications*. 2009; 385:181–186. [PubMed: 19450553]
11. Pakhomov AG, Kolb JF, White JA, Joshi RP, Xiao S, Schoenbach KH. *Bioelectromagnetics*. 2007; 28:655–663. [PubMed: 17654532]
12. Andre FM, Rassokhin MA, Bowman AM, Pakhomov AG. *Bioelectrochemistry*. 2010; 79:95–100. [PubMed: 20097138]
13. Hamill OP, McBride DW Jr. *Pharmacol Rev*. 1996; 48:231–252. [PubMed: 8804105]
14. Lipski J, Park TI, Li D, Lee SC, Trevarton AJ, Chung KK, Freestone PS, Bai JZ. *Brain Res*. 2006; 1077:187–199. [PubMed: 16483552]
15. Li GR, Baumgarten CM. *Am J Physiol Heart Circ Physiol*. 2001; 280:H272–279. [PubMed: 11123242]
16. Palasz A, Czekaj P. *Acta Biochim Pol*. 2000; 47:1107–1114. [PubMed: 11996100]
17. Chanturiya AN, Nikoloshina HV. *The Journal of membrane biology*. 1994; 137:71–77. [PubMed: 7516435]
18. Tanaka T, Li SJ, Kinoshita K, Yamazaki M. *Biochimica et biophysica acta*. 2001; 1515:189–201. [PubMed: 11718674]
19. Ermakov YA, Kamaraju K, Sengupta K, Sukharev S. *Biophysical journal*. 2010; 98:1018–1027. [PubMed: 20303859]
20. Suzuki T, Fujikura K, Higashiyama T, Takata K. *J Histochem Cytochem*. 1997; 45:49–53. [PubMed: 9010468]
21. Pakhomova ON, Gregory BW, Khorokhorina VA, Bowman AM, Xiao S, Pakhomov AG. *PloS one*. 2011; 6:e17100. [PubMed: 21347394]
22. Pakhomova ON, Gregory BW, Pakhomov AG. *Journal of cellular and molecular medicine*. 2013; 17:154–159. [PubMed: 23305510]
23. Ohki S, Duax J. *Biochimica et biophysica acta*. 1986; 861:177–186. [PubMed: 3756152]
24. Mussauer H, Sukhorukov VL, Haase A, Zimmermann U. *The Journal of membrane biology*. 1999; 170:121–133. [PubMed: 10430656]
25. Ermakov YA, Averbakh AZ, Yusipovich AI, Sukharev S. *Biophysical journal*. 2001; 80:1851–1862. [PubMed: 11259298]
26. Sinn CG, Antonietti M, Dimova R. *Colloid Surface A*. 2006; 282:410–419.
27. Alexy T, Nemeth N, Wenby RB, Bauersachs RM, Baskurt OK, Meiselman HJ. *Biorheology*. 2007; 44:361–373. [PubMed: 18401075]
28. Martin-Molina A, Rodriguez-Beas C, Faraudo J. *Physical review letters*. 2010; 104:168103. [PubMed: 20482084]
29. Martin-Molina A, Rodriguez-Beas C, Faraudo J. *Biophysical journal*. 2012; 102:2095–2103. [PubMed: 22824273]
30. Li XM, Zhang YF, Ni JZ, Chen JW, Hwang F. *Journal of inorganic biochemistry*. 1994; 53:139–149. [PubMed: 8133251]
31. Verstraeten SV, Nogueira LV, Schreier S, Oteiza PI. *Arch Biochem Biophys*. 1997; 338:121–127. [PubMed: 9015396]
32. Bentz J, Alford D, Cohen J, Duzgunes N. *Biophysical journal*. 1988; 53:593–607. [PubMed: 3382713]
33. Vernier PT, Ziegler MJ, Dimova R. *Langmuir : the ACS journal of surfaces and colloids*. 2009; 25:1020–1027. [PubMed: 19063658]
34. Tsai HH, Lai WX, Lin HD, Lee JB, Juang WF, Tseng WH. *Biochimica et biophysica acta*. 2012; 1818:2742–2755. [PubMed: 22683599]
35. Akuzawa-Tateyama M, Tateyama M, Ochi R. *The Journal of physiology*. 1998; 513(Pt 3):775–786. [PubMed: 9824717]

36. Levine ZA, Vernier PT. *The Journal of membrane biology*. 2012; 245:599–610. [PubMed: 22815071]
37. Yang XC, Sachs F. *Science*. 1989; 243:1068–1071. [PubMed: 2466333]
38. Iwamoto T, Shigekawa M. *Am J Physiol*. 1998; 275:C423–430. [PubMed: 9688596]
39. Lerner I, Trus M, Cohen R, Yizhar O, Nussinovitch I, Atlas D. *J Neurochem*. 2006; 97:116–127. [PubMed: 16515555]
40. Lansman JB. *J Gen Physiol*. 1990; 95:679–696. [PubMed: 2159974]
41. Mlinar B, Enyeart JJ. *The Journal of physiology*. 1993; 469:639–652. [PubMed: 8271221]
42. Malasics A, Boda D, Valisko M, Henderson D, Gillespie D. *Biochimica et biophysica acta*. 2010; 1798:2013–2021. [PubMed: 20696128]
43. Song YM, Ochi R. *The Journal of physiology*. 2002; 545:463–473. [PubMed: 12456826]
44. Dyachok O, Zhabyeyev P, McDonald TF. *The Journal of membrane biology*. 2010; 238:69–80. [PubMed: 21104181]
45. Wu SN, Huang HC, Yeh CC, Yang WH, Lo YC. *Biochemical and biophysical research communications*. 2011; 405:508–513. [PubMed: 21262200]

Highlights

- Gd^{3+} causes a lasting modification of the cell membrane to inhibit electroporation.
- Gd^{3+} does not clog electropores.
- Modification by Gd^{3+} occurs promptly and independently of electropore presence.
- Gd^{3+} makes the plasma membrane less prone to electropermeabilization.
- Gd^{3+} reduces the size and/or lifetime of formed electropores.

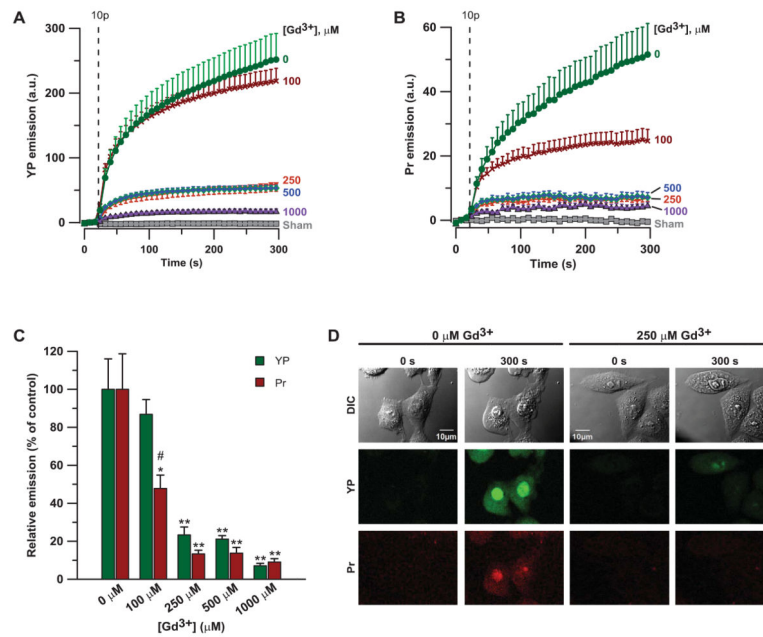


Figure 1. Gd³⁺ inhibits nsEP-induced uptake of YP and Pr in a concentration-dependent manner

CHO-K1 cells bathed with Gd³⁺ at the indicated concentration were subjected to 10, 600-ns, 20 kV/cm pulses at 28 s (dashed line). Sham-exposed cells were not exposed to nsEP and were bathed without Gd³⁺. The emission curves of YP and Pr are shown in panels (A) and (B), respectively. Panel (C) presents the dye emission measurements by the end of experiment (300 s) in percent (%) to the 0 Gd³⁺ group. Mean values \pm s.e. for 4–10 cells in each group. * $p < 0.05$, ** $p < 0.01$ vs. 0 μM Gd³⁺; control; # $p < 0.01$ Pr vs. YP at the same concentration of Gd³⁺. For clarity, error bars are shown in one direction only. (D): Representative DIC and fluorescence images of cells before and after nsEP treatment in the absence (left panels) or presence (right panels) of Gd³⁺.

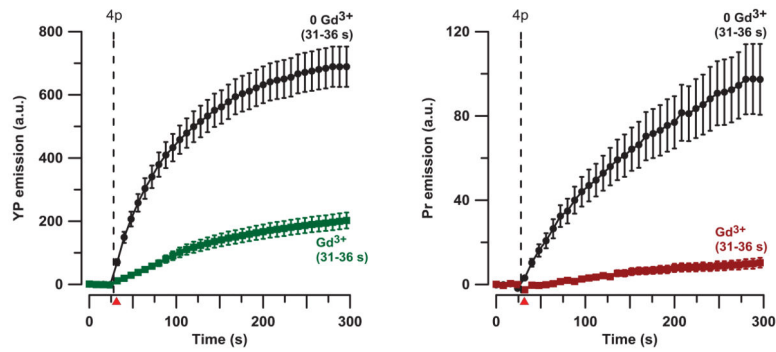


Figure 2. A brief perfusion of Gd^{3+} after nsEP exposure inhibits YP and Pr uptake
 Intact cells were exposed to 4, 600-ns, 20 kV/cm pulses at 28 s (dashed line), followed at 31 s by a 5-s perfusion (red triangle) using a fast-step system (see Methods). The emission curves of YP and Pr are shown in the left and right panels, respectively. Labels next to emission curves indicate which solution was delivered (“0 Gd^{3+} ” is the same solution as in the bath, in order to control for possible mechanical artifacts, and “ Gd^{3+} ” is the bath solution with 250 μM Gd^{3+}) and the time of perfusion (31 to 36 s). Mean \pm s.e. for 25–32 cells in each group. Error bars may be not visible when they are smaller than the central symbol. The inhibitory effect of Gd^{3+} is significant at $p < 0.01$.

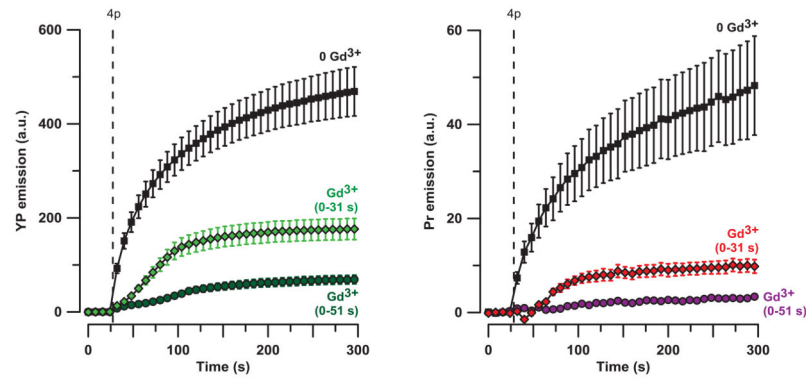


Figure 3. Gd^{3+} present in the solution during nsEP exposure does not prevent pore formation, but the pores remain quiescent

Cells were bathed in the physiological solution with either 0 or 250 μM Gd^{3+} . The vertical dashed line shows the onset of nsEP exposure (4 pulse, 600 ns, 20 kV/cm). In the latter groups, Gd^{3+} was present until immediately after the exposure (0–31 s) or until 20 s after the exposure (0–51 s), at which time the wash by the bath perfusion with Gd^{3+} -free physiological solution began and continued until the end of the experiment. Mean \pm s.e. for 19–24 cells per group. Differences between all groups are significant at $p < 0.01$. Note the cessation of dye uptake in Gd^{3+} -treated cells at about 100 s into the experiment, despite the absence of Gd^{3+} in the solution.

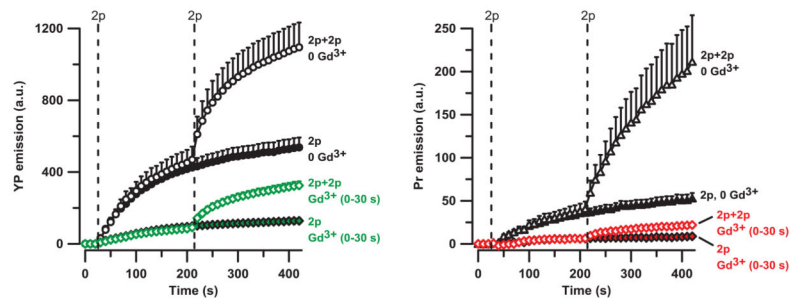


Figure 4. Cells pre-incubated with Gd^{3+} are less vulnerable to permeabilization by subsequent nsEP

Left and right panels show the time course of YP and Pr uptake, respectively. Vertical dashed lines identify the exposures to a pair of 600-ns, 20 kV/cm pulses. Cells were exposed only to the first pair of pulses (2p, filled symbols), or to both pairs (2p+2p groups, open symbols). Gd^{3+} (0–30 s): 250 μM Gd^{3+} were in the solution until after the first nsEP exposure, followed by a wash with Gd^{3+} -free physiological solution until the end of the experiment. 0 Gd^{3+} : control cells not treated with Gd^{3+} at any time. Mean \pm s.e. for 18–23 cells per group. Error bars are shown in one direction only for clarity. Differences between all groups are significant at $p < 0.01$. Note the reduced response to the second nsEP exposure in Gd^{3+} -treated cells, despite the absence of Gd^{3+} in the solution.

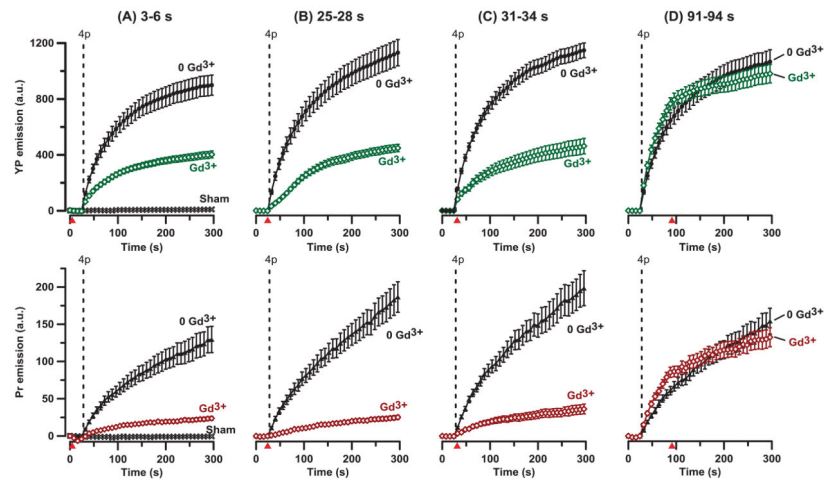


Figure 5. The role of timing of Gd^{3+} perfusion for inhibition of cell permeabilization by nsEP
 Top and bottom panels show the time course of YP and Pr uptake, respectively. Vertical dashed lines identify the exposure to 4, 600-ns, 20 kV/cm pulses at 28 s. Cells were treated with physiological solution containing either 0 or 250 μM Gd^{3+} by a brief 3-s perfusion using a fast step system from A) 3–6 s, B) 25–28 s, C) 31–34 s, or D) 91–94 s (identified by the red arrows over the abscissa). See Figure 2 for more details. Sham exposed cells (shown in A only) were not exposed to either nsEP or Gd^{3+} . Mean \pm s.e. for 13–23 cells per group. The inhibitory effect of Gd^{3+} is significant at $p < 0.01$ in all groups except D. However, note that the difference in the extent of inhibition between panels A, B, and C is not significant.